HHS Public Access

Author manuscript

Brain Behav Immun. Author manuscript; available in PMC 2025 January 01.

Published in final edited form as:

Brain Behav Immun. 2024 January ; 115: 406–418. doi:10.1016/j.bbi.2023.11.002.

Chemogenetic approaches reveal dual functions of microglia in seizures

Aastha Dheer[1], **Dale B. Bosco**[1], **Jiaying Zheng**[1,2], **Lingxiao Wang**[1,2], **Shunyi Zhao**[1,2], **Koichiro Haruwaka**[1], **Min-Hee Yi**[1], **Abhijeet Barath**[1,2], **Dai-Shi Tian**[5], **Long-Jun Wu**[1,3,4,*]

[1]Department of Neurology, Mayo Clinic, Rochester, Minnesota, USA.

[2]Mayo Clinic Graduate School of Biomedical Sciences, Rochester, Minnesota, USA.

[3]Department of Neuroscience, Mayo Clinic, Jacksonville, Florida, USA.

[4]Department of Immunology, Mayo Clinic, Rochester, Minnesota, USA.

[5]Department of Neurology, Tongji Hospital, Tongji Medical College, Huazhong University of Science and Technology, Wuhan 430030, China

Abstract

Microglia are key players in maintaining brain homeostasis and exhibit phenotypic alterations in response to epileptic stimuli. However, it is still relatively unknown if these alterations are pro- or anti-epileptic. To unravel this dilemma, we employed chemogenetic manipulation of microglia using the artificial Gi-Dreadd receptor within a kainic acid (KA) induced murine seizure model. Our results indicate that acute Gi-Dreadd activation with Clozapine-N-Oxide can reduce seizure severity. Additionally, we observed increased interaction between microglia and neuronal soma, which correlated with reduced neuronal hyperactivity. Interestingly, prolonged activation of microglial Gi-Dreadds by repeated doses of CNO over 3 days, arrested microglia in a less active, homeostatic-like state, which associated with increased neuronal loss after KA induced seizures. RNAseq analysis revealed that prolonged activation of Gi-Dreadd interferes with interferon β signaling and microglia proliferation. Thus, our findings highlight the importance of microglial Gi signaling not only during *status epilepticus* (SE) but also within later seizure induced pathology.

Keywords

Microglia; Chemogenetics; Kainic acid; Seizures; Gi-Dreadds; Hippocampus

*Corresponding author: Long-Jun Wu, Ph.D., wu.longjun@mayo.edu, Department of Neurology, Mayo Clinic, 200 First Street SW, Rochester 55905.

Author contributions

A.D. and L.J.W. designed the study and wrote the manuscript. A.D. performed the experiments and collected data. D.B.B assisted with experimental design. J. Z. and S.Z. assisted with RNA sequencing experiments. L.W. performed data mining and RNAseq data analysis. K.H. helped with data analysis. M.H.Y., A.B. and D.T. assisted with manuscript revision.

Declaration of interests

The authors declare no competing interests.

Introduction:

Epilepsy is a brain disorder characterized by recurrent seizures which affects over 50 million people worldwide [1]. Despite the availability of various anti-epileptic drugs (AEDs), one-third epilepsy patients remain refractory to treatment. Since the most of commonly used AEDs preferentially target neuronal mechanisms, it is critical to explore alternative mechanisms to provide better therapeutic strategies [2–5]. Microglia, the immune cells of central nervous system (CNS), are key regulators of brain disease [6, 7]. Microglia can also sense alterations in neuronal signaling via neurotransmitters and neuromodulators and can regulate neuronal functions [8–11].

Accumulating evidence suggests microglia have a significant role in epileptogenesis [5, 12–16] and neuronal death after *status epilepticus* [15, 17–19]. However, whether microglia are protective or neurotoxic in epilepsy is still under debate and likely dependent on spatial and temporal factors. Nevertheless, the protective roles of microglia are being increasingly recognized. For instance, interactions between microglia and neurons have been shown to reduce neuronal firing and seizure severity [5, 20–24]. During acute seizures increased microglial process length in a glutamate dependent manner have been reported [25]. The deletion of the P2Y12 receptor, which is critical for ATP sensing, was shown to aggravate seizures [21, 25]. Disruption of microglial fractalkine signaling was also shown to exacerbate seizures [26]. Moreover, depletion of microglia was shown to aggravate seizures both acutely and the development of spontaneous recurrent seizures [15]. This contrasts with other reports suggesting that depleting microglia reduced deleterious effects [27, 28]. Thus, there is need to fully address this interesting duality of microglia function in epilepsy by precisely targeting microglia within a seizure context.

Novel approaches like chemogenetic manipulations using artificial Designer Receptors Exclusively Activated by Designer Drugs (Dreadd) which enables fine modulation of targeted signaling pathways [29, 30]. The most commonly used Dreadds are the human M3 muscarinic receptor (hM3Dq) which enhances activity via Gq signaling [31] and hM4Di which can silence activity via Gi signaling [30]. The most widely used ligand for these receptors is Clozapine-N-Oxide (CNO), a pharmacologically inert metabolite of Clozapine and an atypical antipsychotic drug (Armbruster et al., 2007; Roth et al., 1994). However, several other compounds like compound 21 [32], perlapine [33], and descholoroclozapine [34] have been designed for increased Dreadd efficacy and specificity.

Previous studies have utilized Dreadd approaches primarily to modulate neuronal activity [35–38]. However, some have utilized chemogenetic approaches within microglia to modulate peripheral-nerve-injury-induced neuropathic pain [39, 40]. Further, recent findings found that microglial Gi-signaling can regulate microglia-neuron interactions and neuronal excitability [41]. Microglia interact with neurons at specialized areas to engage in cell-cell communication [23]. The microglial specific Gi-coupled receptor P2Y12 may have a crucial role in this communication [23, 25]. In the present study we aim to explore the role of microglia in epilepsy by specifically manipulating microglial Gi-signaling using a chemogenetic approach.

Results

Microglial Gi-Dreadd activation reduces seizure severity in the ICV-KA model of epilepsy.

Previous studies have highlighted the protective role of microglia in acute seizure models [5, 15, 25]. However, the mechanism underlying microglial neuroprotection during seizure onset remains largely unknown. To address this question, we used $Cx3cr1^{CreER/WT}$: $R26^{LSL\text{-}hM4Di/WT}$ mice (Gi-Dreadd) which specifically express Gi-Dreadd in microglia under the inducible CX3CR1 promoter. $Cx3cr1^{CreER/WT}$ mice (Control) without Gi-Dreadd expression were used as Controls (Fig. 1A). Fig. 1B illustrates the experimental timeline. Our results revealed that activation of microglial Gi-Dreadd by CNO significantly reduced seizure score ($p < 0.05$) when compared to controls (Fig. 1C, D). To confirm any genotypic differences in susceptibilities to seizures, we additionally performed KA induced seizures without CNO injection in both the control and Gi-Dreadd groups. Our results confirmed that both control and Gi-Dreadd groups had a similar seizure profile when exposed to kainic acid in the absence of CNO, indicating no genotypic differences in seizure susceptibilities (Suppl. Fig. 1A, B, C).

To validate Gi-Dreadd expression, we performed immunostaining for HA (Dreadd tag) in Gi-Dreadd and Control groups. (Fig. 1E). In the absence of tamoxifen injection, no HA expression was observed in Gi-Dreadd mice confirming cre dependent Gi-Dreadd expression (Suppl. Fig. 2A). The results showed the expression of HA positive cells ($p < 0.0001$) was specific to Gi-Dreadd mice (Fig. 1F). Additionally, to observe Gi-Dreadd cellular specificity, sections were co-stained with GFAP, NeuN, and IBA1 markers for astrocyte, neurons, and microglia respectively (Fig. 1G). Indeed, HA expression colocalized with IBA1 staining ($p < 0.0001$) but not with NeuN or GFAP (Fig. 1H).

Furthermore, since Cx3cr1 is also expressed by peripheral macrophages, we wanted to confirm the observed phenotype was specific to microglial Gi-Dreadd activation. As such, we used the $Tmem119^{creER}$ mouse line to express Gi-Dreadd specifically in microglia [42, 43]. Consistently, we observed a significant reduction in seizure score after CNO injection in the Gi-Dreadd mice when compared with controls (Suppl. Fig. 2 B, C). Our results clearly demonstrate that activation of Gi-Dreadd within microglia affects seizures acutely.

Acute Gi-Dreadd activation increases microglia-neuronal interaction and reduces neuronal hyperactivity following seizures.

We next wanted to investigate how Gi-Dreadd activation was affecting microglial behavior. Immunostaining results (Fig. 2A) revealed that Gi-Dreadd activation resulted in increased ($p < 0.05$) $IBA1^+$ cell number (Fig. 2B), and immunoreactivity ($p < 0.01$) (Fig. 2C) within the CA3 region 2 h post-KA. Further, Sholl analysis revealed a significant reduction ($p < 0.0001$) overall microglial process complexity within the Gi-Dreadd group when compared to control (Fig. 2D, E). Soma size was also significantly increased ($p < 0.05$) in Gi-Dreadd microglia (Fig. 2F). In the CA1 region, we observed an increase in $IBA1^+$ area ($p < 0.05$) (Suppl. Fig. 3 A, C), but there was no difference in microglial cell number (Suppl. Fig. 3B) To further characterize microglial alterations, we performed CD68 immunostaining of the CA3 region. The results showed significant ($p < 0.05$) upregulation of CD68 expression

in the Gi-Dreadd group when compared to control (Fig. 2G, H). Together, these results clearly demonstrate that Gi-Dreadd signaling influences microglial activation in response to KA-induced seizures.

To further investigate how microglial Gi-Dreadd activation reduces seizure severity, we examined the interaction between microglia and neurons. Our previous studies found that neuronal hyperactivity after seizures induces microglial process extension towards neuron in the hippocampus [25]. Interestingly, we observed a significant increase ($p < 0.05$) in $IBA1^+$ area overlap with $NeuN^+$ somas in Gi-Dreadd mice after *status epilepticus* when compared to controls (Fig. 2 I, J). To investigate neuronal activity in relation to microglial Gi-Dreadd activation, we analyzed the number of active c-FOS^+ neurons present following KA-induced seizures. The results showed a significant decrease ($p < 0.05$) in c-FOS^+ neurons in the CA3 region of Gi-Dreadd mice when compared to controls (Fig. 2K, L). When investigating the CA1 region we did not observe differences in both microglia-neuron interaction after microglial Gi-Dreadd activation, $cFOS^+$ neuron number (Suppl. Fig. 3D–F). Together, these results indicate that microglial Gi-signaling has a role in regulating microglia-neuron interaction and may be neuroprotective.

Prolonged Gi-Dreadd induction reduces microglia activation and restores homeostatic state.

We next wanted to determine how microglial Gi-Dreadd activation affected post-seizure pathology. As such, we examined tissues collected 3 days post-KA when microglial numbers have been reported to peak [4]. To maintain Gi-Dreadd activation, CNO was injected once daily for three days following KA administration (Fig. 3A). We carried out immunostaining for IBA1 and CD68 (Fig. 3B) in the CA3 region of the hippocampus. The results revealed that upon 3 days after seizures, the number of microglia (Fig. 3C) in Gi-Dreadd group was decreased as compared to control group. Additionally, the soma size for Gi-Dreadd microglia was also reduced as compared to the control microglia (Fig. 3D). Furthermore, the surface area/volume ratio of microglia is higher in Gi-Dreadd group suggesting that they were more ramified as compared to control group (Fig. 3E). The expression of CD68 was also reduced in the Gi-Dreadd group (Fig. 3F), indicating decreased microglial reactivity. These results suggest that microglial Gi-Dreadds activation reduces microglial reactivity after 3 days of KA-induced seizures.

We also looked for microglia proliferation following 3 days of i.c.v.-KA and CNO injections using Ki-67 (marker for proliferating cells) co-labelled with IBA1 (Fig. 3G). The results showed a significant decrease ($p < 0.05$) in no. of proliferating microglial cells in the Gi-Dreadd group as compared to the controls (Fig. 3H). We had similar observations after prolonged CNO induced activation of Gi-Dreadds in mice exhibiting similar seizures profiles following KA injection prior to CNO administration (Suppl. Fig. 1D, E, F, G).

Next, we assessed the expression of P2Y12, a microglial homeostatic marker. Our results revealed a significant downregulation ($p < 0.001$) of P2Y12 following seizure induction when compared to sham controls (Fig. 3I, K, suppl. 4A). Interestingly, P2Y12 down-regulation was significantly suppressed by Gi-Dreadd activation ($p < 0.05$) (Fig. 3I, K). Additionally, we investigated expression of TMEM119, another microglial homeostatic

marker. However, our results revealed that while seizure induction reduced TMEM119 expression, there was not a statistically significant differences between Gi-Dreadd and control groups (Fig. 3J, L).

Finally, we wanted to investigate how microglial Gi Dreadd activation affected monocyte infiltration. It is well established that following *status epilepticus* there is significant infiltration of peripheral monocytes that can have important roles in epilepsy associated neurodegeneration [4, 19, 44]. To address this, we combined TMEM119 and CD169 immunostaining to differentiate microglia from infiltrated macrophages. While our results did confirm infiltration of peripheral macrophages ($p < 0.05$) following KA administration, there was not a statistically significant difference in the number of $CD169^{+}TMEM119^{-}$ cells between groups (Fig. 3J, M, suppl. 4B).

Transcriptomic alterations in microglia upon prolonged activation of Gi-signaling following *status epilepticus*.

We next sought to investigate the underlying mechanisms affected by prolonged Gi-Dreadd activation. To this end, RNA was extracted from the ipsilateral hippocampal $CD11b^{+}$ cells, 3 days post-KA from both control and Gi-Dreadd mice (Fig. 4A). The quality and purity of cells for the RNAseq data is represented with a heatmap depicting TPM expression values for microglia, astrocytes, neurons, endothelial cells, and oligodendrocytes cell specific genes (suppl. 5). RNAseq revealed a total of 69 genes were differentially expressed in the Gi-Dreadd group relative to control group. Differentially expressed genes (DEGs) had an even distribution of chromosome locations (Fig. 4B). We also found that 43 DEGs were down-regulated within Gi-Dreadd activated mice while the remaining 26 were up-regulated (Fig. 4C). The heatmap shows the relative expression level of all DEGs between groups (Fig. 4D, suppl. 6). Of note, the downregulated genes included several interferon-regulated genes. We also observed differential expression of Ace (Angiotensin-converting enzyme), Siglec1 (sialic acid binding Ig like lectin 1), and Mki67, a marker of proliferation. Among the fewer up regulated, the most pertinent ones were Chrm4 (cholinergic receptor muscarinic 4), Tuba1a (Tubulin alpha 1a), Dusp8 (dual specificity phosphatase 8), and lL1α (interleukin 1 alpha) (Fig. 4C, D). Next, we performed Gene Ontology (GO) enrichment analysis (Fig. 4E). In addition to the GO analysis, we performed Gene Set Enrichment Analysis (GSEA), which determined whether the whole transcriptome was significantly different between groups (Table 1). We found that most significantly altered genes were involved in interferon β signaling and microglia proliferation.

Prolonged activation of microglial Gi-signaling during disease progression increases neurodegeneration.

Next, we determined how prolonged microglial Gi-signaling activation affected seizure associated neurodegeneration. We found a significant decrease ($p < 0.05$) in CA3 hippocampal neuronal cell number ($NeuN^{+}$) in the Gi-Dreadd group when compared to the controls (Fig. 5A, B). Additionally, Nissl staining showed a significantly ($p < 0.05$) lower number of healthy, $Nissl^{+}$ cells in the pyramidal layer of the Gi-Dreadd mice (Fig. 5C, D). Consistently, Fluoro-Jade C showed increased neurodegeneration in the Gi-Dreadd group

(Fig. 5E, F). These results indicate that chronic activation of microglial Gi-Dreadd promotes the KA-induced neuronal death.

Since our RNAseq results indicated an increase in the Il-1α expression within the Gi-Dreadd group, we wanted to determine if this contributed to the observed effect upon neurodegeneration. As such, we performed immunostaining for IL-1α. Our results confirmed significant upregulation ($p < 0.05$) in IL-1α expression in the Gi-Dreadd group when compared to the controls (Fig. 5G, H). IL-1α has been previously reported to induce activation of neurotoxic A1 type astrocytes [45], that may contribute to neuronal death. Additionally, we found that inhibiting microglia via Gi-Dreadd did not reduce astrocyte activation as determined by GFAP immunoreactivity between control and Gi-Dreadd groups (Suppl. 7A, B, C), suggesting that astrocytes exhibited an activated phenotype.

Discussion

Mounting evidence describes the importance of microglia in controlling both homeostatic and pathologic brain function. In the epileptic brain, microglia adopt various phenotypes depending on the disease stage and can display both protective and/or deleterious functions [5, 15, 25, 46]. In this study, we are utilizing the novel chemogenetic approach as a tool to explore the function of microglia in epilepsy. Our results reveal that Gi-Dreadd activation reduced seizure severity in mice acutely. Whereas prolonged activation of Gi-Dreadd, arrested microglia in a homeostatic-like state which correlated with increased neuronal loss. Understanding the role of microglia in regulating seizures is crucial to developing potential therapeutic targets to ameliorate seizures. Our current study sheds light on microglial function and provides new avenues for future research.

Acute activation of microglial Gi-signaling dampened seizure severity by increasing microglia-neuronal interactions.

The protective role of microglia in acute seizures has been previously studied by employing genetic deletion and ablation strategies [5, 14–16, 47]. Consistently, our own results also point towards a protective role of microglia. Moreover, another study using a MgPTX mouse line showed that inhibition of Gi signaling in microglia resulted in hypersynchrony and spontaneous seizures [41]. Further, microglia can respond rapidly to acute neuronal hyperactivity [25, 48] and form purinergic junctions to monitor neuronal activity [23]. We also observed increased microglial interaction with the neurons following acute seizures in response to Gi-Dreadd activation. G protein-coupled receptor activation has been linked with cytoskeletal rearrangement [49, 50], identifying the critical function of Rho-GTPases in actin remodeling [51]. Therefore, activation of Gi-Dreadd may contribute to cytoskeletal rearrangement and increased microglial process interaction immediately following *SE*. Our results also indicated that activation of microglial Gi-signaling reduced *SE*-induced neuronal excitability. We hypothesize that this microglial regulation may be related to the production of adenosine mediated by microglia and associated suppression of neuronal activity by the adenosine receptor 1 as reported recently [21]. Furthermore, a recent study showed using the adenosine sensor $GRAB_{ADO}$ that CNO-induced Gi activation in microglia leads to increased adenosine which supports our proposed mechanism[52]. Additionally, they reported that Gi

activation increases microglia Ca^{2+} activity [52], increased Ca^{2+} activity has previously been reported to regulate chemotaxis in microglia [38]. Our current study supports the role of Gi-induced acute microglial activation in reducing seizures.

Chronic Gi-Dreadd stimulation inhibits microglial activation following KA induced seizures.

Microglia possess both neurotoxic and neuroprotective functions [53] which greatly depend on the precise timing and context of disease [5, 54]. Curiously, when we investigated the effect of sustained Gi-Dreadd activation within microglia we found, opposite to what we observed immediately following *SE*, microglial reactivity was reduced. These results are consistent with our previous study within the context of neuropathic pain where repeated Gi-Dreadd stimulation reduced microglial activation [40]. Likewise, Binning *et al* describe the opposing effects during acute and chronic activation of Gq-Dreadd in microglial cells, showing that acute activation of Gq in microglia increased pro-inflammatory cytokine production, while this was inhibited by chronic activation [55]. Interestingly, we observed that expression of the homeostatic marker P2Y12 was elevated in the Gi-Dreadd group after *SE* when compared to controls. As such, we can conclude that chronic Gi-signaling stimulation reduces activation of microglia and locks them into a more homeostatic state. However, further studies are needed to explore the possible mechanism in this regard.

Gi signaling could regulate downstream pathways mediated by Gi-coupled receptors like P2Y12 [56] and adenosine 1 receptor [57]. Interestingly, GO analysis highlighted the involvement of genes associated with interferon beta (IFN-β) in our study. Prior literature indicates that microglia are sensitized to IFN-β following KA induced seizures [17]. Moreover, IFN-β has been shown to regulate microglial function in multiple sclerosis [58], highlighting an anti-inflammatory role of IFN-β [59]. However, there are also clues that blocking type-I interferons may be beneficial to brain aging [60]. Additionally, our results highlight elevated IL-1α levels in the Gi-Dreadd group compared to controls. IL-1α is a pro-inflammatory cytokine [61] and has been previously reported to be an inducer for astrocytes [45]. Our results confirm the upregulated immunoreactivity of IL-1α in the Gi-Dreadd group. This could be a potential mechanism for microglia mediated astrocyte activation which warrants further exploration.

Previous investigations have shown increased production of IL-1β after the focal KA application in a rat hippocampus [12]. Additionally, enhanced mRNA levels of IL-1beta, IL-6, and tumor necrosis factor (TNF)-alpha were reported to peak 6 hours after intrahippocampal injection of KA [62]. However, we did not observe any significant differences in IL-1β expression at 2hrs following microglial Gi-Dreadd activation during SE (data not shown), this could be due to the early timepoint of our study. In addition, our RNAseq data did not indicate a significant difference in IL-1β after prolonged Gi-Dreadd activation of microglia following SE. Interestingly, previous study reports prolonged microglial Gi-Dreadd activation reduced microglial activation and IL-1β expression in the spinal cord after peripheral nerve injury [40]. The discrepancy could be due to the regional differences (hippocampus vs. spinal cord) or different diseases context (seizures vs. neuropathic pain).

We observed reduced microglia cell density following prolonged Gi-Dreadd activation. Our immunostaining results as well as RNAseq data are in accordance with these findings. Lower Mki67 levels are indicative of reduced proliferation of microglia in the Gi-Dreadd group. Additionally, increased expression of Tuba1a gene was observed in the Gi-Dreadd group as compared to the controls. Tuba1a gene encodes for the microtubule protein α-Tubulin which is essential for cytoskeleton organization and cell motility in neurons [63–65]. This supports our observation of a more ramified morphology of microglia after chronic Gi-activation. Additionally, the significant upregulation of chrm4 (cholinergic receptor muscarinic 4) in Gi-Dreadd microglia confirmed the specificity and success of the genetic mouse line for microglia specific Gi-Dreadd as compared to control microglia [30].

Microglia inhibition during disease progression is detrimental to neuronal survival.

Finally, our results suggest that arresting microglia in a homeostatic state following seizures may have a detrimental effect on neuronal health. Similarly, we found loss of TREM2 locked microglia in homeostatic states that impairs microglial protective functions in TDP-43 neurodegeneration [66]. Microglia have roles as the resident CNS immune cells, such as the removal of cell debris, and cytokine release (Sierra et al., 2010). Additionally, microglia increase expression of CD68, phagocytic function, after SE which prevents the formation of hyperexcitable aberrant neural circuits [67]. We observed reduced CD68 immunoreactivity following Gi-Dreadd activation indicating impaired removal of abnormal cells and debris. It should be noted that other cells like infiltrating monocytes [44, 68] and astrocytes also play roles in neuroinflammation and neuronal death [69]. In our study we report that there was comparable monocyte infiltration and astrocyte cell density in relation to Gi-Dreadd activation with control group. To end, it is worth considering that microglial activation in the acute phase may also contribute towards neuronal clearance in the Gi-Dreadd group as an initial response.

Lastly, it is pertinent to describe the limitations in the chemogenetic manipulations highlighted in this study. The metabolite of CNO, clozapine is a commonly used antipsychotic drug which has been shown to target few endogenous dopaminergic receptors, serotonergic receptors, H1 histamine receptors and adrenergic receptors, which may result in some to off-target effects of the drug [70, 71]. The feasibility of CNO drug has been argued recently due to the potential off-target effects of its metabolite clozapine [72]. This potential caveat may best be overcomed by using appropriate control groups of non-Dreadd animals treated with CNO, which we employed in our study [73]. Alternatively, other compounds like Deschloroclozapine and Compound 21 reported to be more potent, may be utilized [34, 74]. Despite the limitations, the chemogenetic approach is an impressive neuroscience tool that provides a precise way of manipulating specific cell types.

In our study we use this powerful yet evolving technique to explore microglia function in epilepsy for the first time. Our findings highlight a dual function for microglia Gi-signaling in epilepsy. Acute activation of microglia Gi-Dreadd reduces neuronal activity supporting the protective function of microglia activation in epilepsy, while sustained activation of Gisignaling results in microglial arrest which has detrimental outcomes. Our study strengthens the idea that microglial regulation in epilepsy is bi-phasic, thus opening

exciting new avenues of epilepsy research with future studies designed using chronic models like IH-KA or IA-KA to explore the function of microglia in development of spontaneous recurrent seizures or epileptogenesis.

Materials and Methods:

Animal model:

Cx3cr1$^{CreER/WT}$ (Control) and Cx3cr1$^{CreER/WT}$: R26$^{LSL\text{-}hM4Di/WT}$ (Gi-Dreadd) mice were used for the study. The Cx3cr1$^{CreER/WT}$ mice were generated by crossing C57BL/6J with Cx3cr1$^{CreER/CreER}$ (021160) mice [75]. For generating Cx3cr1$^{CreER/WT}$: R26$^{LSL\text{-}hM4Di/WT}$ mice, homozygous R26$^{LSL\text{-}hM4Di}$ (026219) [76] were crossed with Cx3cr1CreER/CreER. Tmem119 CreER/WT: R26LSL-hM4Di/WT were generated by breeding Tmem119$^{CreER/CreER}$ (031820) mice with R26$^{LSL\text{-}hM4Di\ /hM4Di}$ mice. All mouse lines were obtained from the Jackson Laboratory, and then bred at Mayo Clinic. Age matched 8- to 10-week-old, male mice were used for the study in accordance with the institutional guidelines approved by animal care and use committee at Mayo Clinic.

Randomization and blinding:

Mice were grouped according to the genotype before they were randomly assigned to the experimental groups for sham and seizure experiments. For seizure scoring, one investigator was blinded to the genotype during data collection.

Gi-Dreadd expression and activation:

All injection paradigms were same for both the groups. In this transgenic model Gi-Dreadd expression is controlled by tamoxifen inducible Cre expression under the microglial Cx3cr1. To induce the expression of Cre recombinase, tamoxifen (150 mg/kg) in corn oil (20 mg/mL) was injected intraperitoneally (i.p.) once per day, alternating every 2 days for a total of 4 doses. The Cx3cr1 receptor is mainly expressed in microglia but also expressed by other immune cells like macrophages [77]. Since monocytes have a fast turnover rate [75, 78], all experiments were performed after 28 days of tamoxifen injection to allow only resident microglia specific Gi-Dreadd expression. For the Tmem119 promoter induced Gi-Dreadd mouse model, experiments were performed seven days after tamoxifen injection. Clozapine-N-Oxide (CNO, Cayman Chemicals, Cat. No. 16882) was injected (i.p.) at a dose of 5 mg/kg body weight to activate Gi-Dreadds.

Intracerebroventricular (i.c.v.) surgery:

The icv-KA-induced seizure model was used as described previously (Eyo et al., 2014; Eyo et al., 2015). Briefly, mice were anesthetized with isoflurane and using stereotaxic surgery, a 26-gauge, stainless steel guide cannula was implanted into the intracerebroventricular (ICV) space using the following coordinates (−0.2 mm anteroposterior (AP), +1.0 mm mediolateral (ML), −2.0 mm dorsoventral (DV) from bregma. Mice underwent post-operative recovery for 5 days, before seizure induction.

Drug administration:

Intracerebroventricular (i.c.v.) injection of kainic acid (Tocris, cat. No. 0222) 0.15 μg in 5 μL sterile PBS was administered as previously described [4, 19, 25]. KA was administered i.c.v. *via* the guide cannula using a 20-μL Hamilton syringe attached to a 30-guage needle (Becton Dickinson, Franklin Lakes, NJ, USA) with a polyethylene PE20 tube (Plastics One, Roanoke, VA, USA). The solution was gradually injected over a period of one minute and the needle was removed after an additional two minutes to prevent reflux from the cannula. Sterile PBS was administered as a vehicle for the control injection. Seizures were scored as per the modified Racine scale [79, 80] as described in the next para. Following seizure onset, CNO (5 mg/kg body weight, i.p.) was administered 20 minutes after KA injection to mice that had an onset score higher than 3, and seizure scores were recorded.

Characterization of behavioral seizures:

Seizure behavior was monitored using a modified Racine scale: (1) freezing behavior; (2) rigid posture with raised tail; (3) continuous head bobbing and forepaws shaking; (4) rearing, falling, and jumping; (5) continuous level 4; and (6) loss of posture and generalized convulsion activity [79, 80].

Seizure Score:

Each animal was scored according to the behavioral manifestation observed during a 2 h period. The scores were recorded every 5mins, until 120min. The time-dependent response is represented in Fig. 1B, Suppl. Fig1B, Suppl. Fig. 2B. The seizure scores during the 2hrs duration was averaged for each animal to determine the average seizure scores as represented in Fig. 1C, Suppl Fig. 1C and Suppl. Fig. 2C.

Fluorescent immunostaining:

The procedures were described previously (Mo et al., 2019). Briefly, brain samples were collected after transcardial perfusion of deeply anesthetized mice with ice cold PBS followed by 4% PFA. 30 μm slices were cut using a cryostat (Leica CM1520). Immunostaining was performed on floating sections. Sections were washed with PBS, incubated in 0.25% triton X-100 for 45min at RT. Next, sections were blocked with appropriate serum and incubated with primary antibodies as listed in table 2, overnight at 4C, followed by appropriate secondary antibody incubation at RT for an hour. After vigorous washing, sections were mounted using DAPI containing fluoromount-G mounting medium (SouthernBiotech, Birmingham, AL). Fluorescent images were collected using the LSM980 confocal microscope (Carl Zeiss Microscopy, LLC). Z-stacked images were collected. Analysis was performed with unbiased stereology.

Microglia-neuronal soma interaction analyses:

High-magnification fluorescent images were collected with oil-immersion 63X lens of LSM980 confocal microscope (Carl Zeiss Microscopy, LLC). Z-stacked images, with 0.5μm interval were taken. Fluorescence signal intensity was quantified using ImageJ software (National Institutes of Health, Bethesda, MD). For unbiased analysis, the channels were split using the split-channels command and only the channel for NeuN was used. Region

of interest (ROI) was drawn around each neuronal soma carefully to surround the periphery using the polygonal selection tool. 20 ROIs per mouse were drawn. Therefore, 100 ROIs were analyzed for each group. The ROIs were then overlayed onto the IBA-1 channel and the IBA-1^{+} area within each ROI was measured.

Nissl staining (cresyl violet):

Morphology of the neurons was observed by Nissl staining. The cresyl violet acetate solution is frequently used to stain Nissl substance in the cytoplasm of neurons in PFA or formalin-fixed tissue. 30 μm coronal sections from each group were air dried at room temperature overnight and processed for Nissl staining. Once rinsed with distilled water, sections were stained in 0.1% cresyl violet staining solution for 2–3 min, dehydrated using alcohol gradient of concentration of 50%, 70% and 100%, followed by clearing with xylene. Sections were then mounted using DPX mounting medium (VWR, Hatfield, PA). Light microscopy was performed using the BZ-X800 Keyence microscope (Keyence corporation of America, Itasca, IL, USA) to evaluate the morphology of the cells in CA3 region of hippocampus for both control and Gi-Dreadd groups after 3 days of i.c.v. KA induced seizures. The small-sized, dense, irregular-shaped pyknotic cells were considered as non-viable neurons.

Fluoro jade C (FJC) staining:

FJC is a poly anionic fluorescence derivative that binds with degenerating neurons with high sensitivity. The sections were stained with FJC solution (AG325, Millipore-Sigma, Burlington, MA) in 0.1% acetic acid for 30 min. The protocol followed as per user manual with slight modifications. Briefly, the sections were washed twice with distilled water and then immersed in 1% NaOH in 80% alcohol for 5 min followed by a further immersion in 70% alcohol for 2 min and then washed in distilled water for 2 min. Freshly prepared 0.06% potassium permanganate solution was added in each section for 15–30 min and gently shaken on a rotating platform. After one wash with distilled water, sections were transferred to FJC (0.0001% working solution) staining solution for 30 min in the dark, followed by subsequent washes with distilled water (1 min each). Excess water from the slides was drained off and the slides were quickly air dried on hot plate at ~50 °C. The slides were then cleared in xylene solution and mounted in DPX mounting media (VWR, Hatfield, PA). Sections were visualized using a suitable filter system for visualizing fluorescein or FITC in the microscope (LSM 780, Carl Zeiss Microscopy, LLC). A bright green fluorescence signal indicated degenerating neurons.

Microglia isolation and RNA extraction:

Following PBS perfusion, brains from 8 weeks old mice were isolated and the ipsilateral hippocampus was extracted for microglia isolation. 3–4 hippocampi were pooled together, and 4 sets were obtained. Microglia were isolated with the magnetic CD11b cell sorting using MACS Adult Brain Dissociation kit (order no. 130–107-677, Miltenyi Biotech, Germany) as per manual instructions. Thereafter, RNA was extracted using RNeasy microkit (Qiagen, Cat. No. 74004). RNA purity and integrity was assessed, and samples were sent out for RNA sequencing to BGI company (BGI Genomics, Shenzhen, China).

Bulk RNA sequencing and data analysis:

Raw sequencing data was first filtered by the SOAPnuke software [81] for quality control purpose. Clean reads were then aligned to the *mus musculus GRCm38.p6* reference genome by the HISAT2 software [82]. Bowtie2 software was used to align clean reads to reference genes for quantification [83]. Differentially expressed genes (DEGs) between the Gi and the control group were calculated by the DESeq2 software [84]. A threshold of $p.adj < 0.05$ and $|log2\ fold\text{-}change| > 0.5$ was used to determine DEGs between conditions. Circlize software was used for the circular visualization of DEGs onto the representative genome diagram [85]. ClusterProfiler software was used for the Gene Ontology (GO) pathway enrichment analysis and the Gene Set Enrichment Analysis (GSEA)[86].

Statistical analyses:

All statistical analysis was performed with GraphPad Prism software (version 10). G*Power v3.1.9.4 power analysis was performed to determine appropriate sample size. Statistical details of the experiments, including sample sizes and statistical tests are described in figure legends. Categorical data such as cell counts were analyzed by non-parametric, Mann-Whitney U test. For non-categorical data, comparison of two groups was performed using a two-tailed unpaired Student's *t*-test. Data is represented as median with interquartile range, *p < 0.05, ** p < 0.01, *** p < 0.001 or ns: non-significant.

Supplementary Material

Refer to Web version on PubMed Central for supplementary material.

Acknowledgments

This work was supported by the following grants from the National Institutes of Health: R35NS132326 (L.-J.W.), R01NS088627 (L.-J.W.) and R01NS112144 (L.-J.W.).

REFERENCES:

1. Thurman DJ, et al. , Standards for epidemiologic studies and surveillance of epilepsy. Epilepsia, 2011. 52 Suppl 7: p. 2–26. [PubMed: 21899536]
2. Kuo CC, et al. , Carbamazepine inhibition of neuronal Na+ currents: quantitative distinction from phenytoin and possible therapeutic implications. Mol Pharmacol, 1997. 51(6): p. 1077–83. [PubMed: 9187275]
3. Schumacher TB, et al. , Effects of phenytoin, carbamazepine, and gabapentin on calcium channels in hippocampal granule cells from patients with temporal lobe epilepsy. Epilepsia, 1998. 39(4): p. 355–63. [PubMed: 9578025]
4. Feng L, et al. , Microglial proliferation and monocyte infiltration contribute to microgliosis following status epilepticus. Glia, 2019. 67(8): p. 1434–1448. [PubMed: 31179602]
5. Eyo UB, Murugan M, and Wu LJ, Microglia-Neuron Communication in Epilepsy. Glia, 2017. 65(1): p. 5–18. [PubMed: 27189853]
6. Avignone E, et al. , Status epilepticus induces a particular microglial activation state characterized by enhanced purinergic signaling. J Neurosci, 2008. 28(37): p. 9133–44. [PubMed: 18784294]
7. Vezzani A, et al. , The role of inflammation in epilepsy. Nat Rev Neurol, 2011. 7(1): p. 31–40. [PubMed: 21135885]
8. Färber K and Kettenmann H, Functional role of calcium signals for microglial function. Glia, 2006. 54(7): p. 656–65. [PubMed: 17006894]

9. Krabbe G, et al. , Activation of serotonin receptors promotes microglial injury-induced motility but attenuates phagocytic activity. Brain Behav Immun, 2012. 26(3): p. 419–28. [PubMed: 22198120]
10. Li Y, et al. , Reciprocal Regulation between Resting Microglial Dynamics and Neuronal Activity In Vivo. Developmental Cell, 2012. 23(6): p. 1189–1202. [PubMed: 23201120]
11. York EM, Bernier LP, and MacVicar BA, Microglial modulation of neuronal activity in the healthy brain. Dev Neurobiol, 2018. 78(6): p. 593–603. [PubMed: 29271125]
12. Vezzani A, et al. , Interleukin-1beta immunoreactivity and microglia are enhanced in the rat hippocampus by focal kainate application: functional evidence for enhancement of electrographic seizures. J Neurosci, 1999. 19(12): p. 5054–65. [PubMed: 10366638]
13. Di Nunzio M, et al. , Microglia proliferation plays distinct roles in acquired epilepsy depending on disease stages. Epilepsia, 2021. 62(8): p. 1931–1945. [PubMed: 34128226]
14. Mo M, et al. , Microglial P2Y12 Receptor Regulates Seizure-Induced Neurogenesis and Immature Neuronal Projections. The Journal of neuroscience: the official journal of the Society for Neuroscience, 2019. 39(47): p. 9453–9464. [PubMed: 31597724]
15. Wu W, et al. , Microglial depletion aggravates the severity of acute and chronic seizures in mice. Brain Behav Immun, 2020. 89: p. 245–255. [PubMed: 32621847]
16. Umpierre AD and Wu LJ, How microglia sense and regulate neuronal activity. Glia, 2020.
17. Bosco DB, et al. , RNAseq analysis of hippocampal microglia after kainic acid-induced seizures. Molecular Brain, 2018. 11(1): p. 34. [PubMed: 29925434]
18. Matsuda T, et al. , TLR9 signalling in microglia attenuates seizure-induced aberrant neurogenesis in the adult hippocampus. Nature communications, 2015. 6: p. 6514–6514.
19. Tian D-S, et al. , Chemokine CCL2-CCR2 Signaling Induces Neuronal Cell Death via STAT3 Activation and IL-1β Production after Status Epilepticus. The Journal of neuroscience: the official journal of the Society for Neuroscience, 2017. 37(33): p. 7878–7892. [PubMed: 28716963]
20. Akiyoshi R, et al. , Microglia Enhance Synapse Activity to Promote Local Network Synchronization. eNeuro, 2018. 5(5): p. ENEURO.0088–18.2018.
21. Badimon A, et al. , Negative feedback control of neuronal activity by microglia. Nature, 2020. 586(7829): p. 417–423. [PubMed: 32999463]
22. Kato G, et al. , Microglial Contact Prevents Excess Depolarization and Rescues Neurons from Excitotoxicity. eNeuro, 2016. 3(3).
23. Cserép C, et al. , Microglia monitor and protect neuronal function through specialized somatic purinergic junctions. Science, 2020. 367(6477): p. 528. [PubMed: 31831638]
24. Li Y, et al. , Reciprocal regulation between resting microglial dynamics and neuronal activity in vivo. Dev Cell, 2012. 23(6): p. 1189–202. [PubMed: 23201120]
25. Eyo UB, et al. , Neuronal hyperactivity recruits microglial processes via neuronal NMDA receptors and microglial P2Y12 receptors after status epilepticus. The Journal of neuroscience: the official journal of the Society for Neuroscience, 2014. 34(32): p. 10528–10540. [PubMed: 25100587]
26. Eyo UB, et al. , Regulation of Physical Microglia–Neuron Interactions by Fractalkine Signaling after Status Epilepticus. eneuro, 2016. 3(6): p. ENEURO.0209–16.2016.
27. Bhandare AM, et al. , Inhibition of microglial activation with minocycline at the intrathecal level attenuates sympathoexcitatory and proarrhythmogenic changes in rats with chronic temporal lobe epilepsy. Neuroscience, 2017. 350: p. 23–38. [PubMed: 28323007]
28. Wang N, et al. , Minocycline inhibits brain inflammation and attenuates spontaneous recurrent seizures following pilocarpine-induced status epilepticus. Neuroscience, 2015. 287: p. 144–56. [PubMed: 25541249]
29. Armbruster BN, et al. , Evolving the lock to fit the key to create a family of G protein-coupled receptors potently activated by an inert ligand. Proceedings of the National Academy of Sciences of the United States of America, 2007. 104(12): p. 5163–5168. [PubMed: 17360345]
30. Urban DJ and Roth BL, DREADDs (Designer Receptors Exclusively Activated by Designer Drugs): Chemogenetic Tools with Therapeutic Utility. Annual Review of Pharmacology and Toxicology, 2015. 55(1): p. 399–417.
31. Alexander G, et al. , Remote Control of Neuronal Activity in Transgenic Mice Expressing Evolved G Protein-Coupled Receptors. Neuron, 2009. 63: p. 27–39. [PubMed: 19607790]

32. Thompson KJ, et al. , DREADD Agonist 21 Is an Effective Agonist for Muscarinic-Based DREADDs in Vitro and in Vivo. ACS Pharmacol Transl Sci, 2018. 1(1): p. 61–72. [PubMed: 30868140]
33. Roth BL, DREADDs for Neuroscientists. Neuron, 2016. 89(4): p. 683–694. [PubMed: 26889809]
34. Nagai Y, et al. , Deschloroclozapine, a potent and selective chemogenetic actuator enables rapid neuronal and behavioral modulations in mice and monkeys. Nat Neurosci, 2020. 23(9): p. 1157–1167. [PubMed: 32632286]
35. Saloman JL, et al. , Gi-DREADD Expression in Peripheral Nerves Produces Ligand-Dependent Analgesia, as well as Ligand-Independent Functional Changes in Sensory Neurons. J Neurosci, 2016. 36(42): p. 10769–10781. [PubMed: 27798132]
36. Koga K, et al. , Chemogenetic silencing of GABAergic dorsal horn interneurons induces morphine-resistant spontaneous nocifensive behaviours. Scientific Reports, 2017. 7(1): p. 4739. [PubMed: 28680103]
37. Ilg A-K, et al., Behavioral Effects of Acute Systemic Low-Dose Clozapine in Wild-Type Rats: Implications for the Use of DREADDs in Behavioral Neuroscience. 2018. 12(173).
38. Umpierre AD, et al. , Microglial calcium signaling is attuned to neuronal activity in awake mice. Elife, 2020. 9.
39. Grace PM, et al. , DREADDed microglia in pain: Implications for spinal inflammatory signaling in male rats. Experimental Neurology, 2018. 304: p. 125–131. [PubMed: 29530713]
40. Yi MH, et al. , Chemogenetic manipulation of microglia inhibits neuroinflammation and neuropathic pain in mice. Brain Behav Immun, 2020.
41. Merlini M, et al. , Microglial Gi-dependent dynamics regulate brain network hyperexcitability. Nature Neuroscience, 2021. 24(1): p. 19–23. [PubMed: 33318667]
42. Tobias K and Guoping F, Tmem119-EGFP and Tmem119-CreERT2 Transgenic Mice for Labeling and Manipulating Microglia. eneuro, 2019. 6(4): p. ENEURO.0448–18.2019.
43. Bennett ML, et al., New tools for studying microglia in the mouse and human CNS. 2016. 113(12): p. E1738–E1746.
44. Varvel NH, et al. , Infiltrating monocytes promote brain inflammation and exacerbate neuronal damage after status epilepticus. Proc Natl Acad Sci U S A, 2016. 113(38): p. E5665–74. [PubMed: 27601660]
45. Liddelow SA, et al. , Neurotoxic reactive astrocytes are induced by activated microglia. Nature, 2017. 541(7638): p. 481–487. [PubMed: 28099414]
46. Morin-Brureau M, et al. , Microglial phenotypes in the human epileptic temporal lobe. Brain, 2018. 141(12): p. 3343–3360. [PubMed: 30462183]
47. Gibbs-Shelton S, et al. , Microglia play beneficial roles in multiple experimental seizure models. Glia, 2023.
48. Eyo UB, et al. , The GluN2A Subunit Regulates Neuronal NMDA receptor-Induced Microglia-Neuron Physical Interactions. Scientific reports, 2018. 8(1): p. 828–828. [PubMed: 29339791]
49. Ganguly S, Saxena R, and Chattopadhyay A, Reorganization of the actin cytoskeleton upon G-protein coupled receptor signaling. Biochimica et Biophysica Acta (BBA) - Biomembranes, 2011. 1808(7): p. 1921–1929. [PubMed: 21501584]
50. Ma AD, et al. , Cytoskeletal reorganization by G protein-coupled receptors is dependent on phosphoinositide 3-kinase gamma, a Rac guanosine exchange factor, and Rac. Mol Cell Biol, 1998. 18(8): p. 4744–51. [PubMed: 9671484]
51. Hall A, Rho GTPases and the actin cytoskeleton. Science, 1998. 279(5350): p. 509–14. [PubMed: 9438836]
52. Chenyan M, et al. , Microglia Regulate Sleep via Calcium-Dependent Modulation of Norepinephrine Transmission. bioRxiv, 2023: p. 2023.07.24.550176.
53. Ransohoff RM and Perry VH, Microglial physiology: unique stimuli, specialized responses. Annu Rev Immunol, 2009. 27: p. 119–45. [PubMed: 19302036]
54. Block ML, Zecca L, and Hong JS, Microglia-mediated neurotoxicity: uncovering the molecular mechanisms. Nat Rev Neurosci, 2007. 8(1): p. 57–69. [PubMed: 17180163]

55. Binning W, et al., Chronic hM3Dq signaling in microglia ameliorates neuroinflammation in male mice. 2020. 88: p. 791–801.
56. Sasaki Y, et al. , Selective expression of Gi/o-coupled ATP receptor P2Y12 in microglia in rat brain. Glia, 2003. 44(3): p. 242–50. [PubMed: 14603465]
57. Draper-Joyce CJ, et al. , Structure of the adenosine-bound human adenosine A1 receptor–Gi complex. Nature, 2018. 558(7711): p. 559–563. [PubMed: 29925945]
58. Kawanokuchi J, et al. , Effects of interferon-beta on microglial functions as inflammatory and antigen presenting cells in the central nervous system. Neuropharmacology, 2004. 46(5): p. 734–742. [PubMed: 14996551]
59. Limmroth V, Putzki N, and Kachuck NJ, The interferon beta therapies for treatment of relapsing-remitting multiple sclerosis: are they equally efficacious? A comparative review of open-label studies evaluating the efficacy, safety, or dosing of different interferon beta formulations alone or in combination. Ther Adv Neurol Disord, 2011. 4(5): p. 281–96. [PubMed: 22010041]
60. Baruch K, et al. , Aging. Aging-induced type I interferon response at the choroid plexus negatively affects brain function. Science, 2014. 346(6205): p. 89–93. [PubMed: 25147279]
61. Di Paolo NC and Shayakhmetov DM, Interleukin 1α and the inflammatory process. Nat Immunol, 2016. 17(8): p. 906–13. [PubMed: 27434011]
62. Vezzani A, et al. , Functional role of inflammatory cytokines and antiinflammatory molecules in seizures and epileptogenesis. Epilepsia, 2002. 43 Suppl 5: p. 30–5. [PubMed: 12121291]
63. Buscaglia G, et al., Bridging the Gap: The Importance of TUBA1A α-Tubulin in Forming Midline Commissures. 2022. 9.
64. Aiken J, et al., The α-Tubulin gene TUBA1A in Brain Development: A Key Ingredient in the Neuronal Isotype Blend. 2017. 5(3): p. 8.
65. Hoogenraad CC and Bradke F, Control of neuronal polarity and plasticity – a renaissance for microtubules? Trends in Cell Biology, 2009. 19(12): p. 669–676. [PubMed: 19801190]
66. Xie M, et al., Microglial TREM2 in amyotrophic lateral sclerosis. 2022. 82(1): p. 125–137.
67. Luo C, Koyama R, and Ikegaya Y, Microglia engulf viable newborn cells in the epileptic dentate gyrus. Glia, 2016. 64(9): p. 1508–17. [PubMed: 27301702]
68. Vinet J, et al. , Microglia are less pro-inflammatory than myeloid infiltrates in the hippocampus of mice exposed to status epilepticus. Glia, 2016. 64(8): p. 1350–62. [PubMed: 27246930]
69. Vezzani A, et al. , Astrocytes in the initiation and progression of epilepsy. Nature Reviews Neurology, 2022. 18(12): p. 707–722. [PubMed: 36280704]
70. Goutaudier R, et al. , DREADDs: The Power of the Lock, the Weakness of the Key. Favoring the Pursuit of Specific Conditions Rather than Specific Ligands. eNeuro, 2019. 6(5).
71. Martinez VK, et al., Off-Target Effects of Clozapine-N-Oxide on the Chemosensory Reflex Are Masked by High Stress Levels. 2019. 10.
72. Gomez JL, et al. , Chemogenetics revealed: DREADD occupancy and activation via converted clozapine. Science, 2017. 357(6350): p. 503–507. [PubMed: 28774929]
73. Mahler SV and Aston-Jones G, CNO Evil? Considerations for the Use of DREADDs in Behavioral Neuroscience. Neuropsychopharmacology, 2018. 43(5): p. 934–936. [PubMed: 29303143]
74. Jendryka M, et al. , Pharmacokinetic and pharmacodynamic actions of clozapine-N-oxide, clozapine, and compound 21 in DREADD-based chemogenetics in mice. Scientific Reports, 2019. 9(1): p. 4522. [PubMed: 30872749]
75. Parkhurst Christopher N., et al. , Microglia Promote Learning-Dependent Synapse Formation through Brain-Derived Neurotrophic Factor. Cell, 2013. 155(7): p. 1596–1609. [PubMed: 24360280]
76. Zhu H, et al., Cre-dependent DREADD (Designer Receptors Exclusively Activated by Designer Drugs) mice. Genesis (New York, N.Y.: 2000), 2016. 54(8): p. 439–446. [PubMed: 27194399]
77. Jung S, et al. , Analysis of Fractalkine Receptor CX₃CR1 Function by Targeted Deletion and Green Fluorescent Protein Reporter Gene Insertion. Molecular and Cellular Biology, 2000. 20(11): p. 4106. [PubMed: 10805752]
78. Peng J, et al. , Microglial P2Y12 receptor regulates ventral hippocampal CA1 neuronal excitability and innate fear in mice. Mol Brain, 2019. 12(1): p. 71. [PubMed: 31426845]

79. Avignone E, et al. , Status Epilepticus Induces a Particular Microglial Activation State Characterized by Enhanced Purinergic Signaling. The Journal of Neuroscience, 2008. 28(37): p. 9133. [PubMed: 18784294]

80. Racine RJ, Modification of seizure activity by electrical stimulation: I. after-discharge threshold. Electroencephalography and Clinical Neurophysiology, 1972. 32(3): p. 269–279. [PubMed: 4110396]

81. Chen Y, et al. , SOAPnuke: a MapReduce acceleration-supported software for integrated quality control and preprocessing of high-throughput sequencing data. Gigascience, 2018. 7(1): p. 1–6.

82. Kim D, et al. , Graph-based genome alignment and genotyping with HISAT2 and HISAT-genotype. Nature Biotechnology, 2019. 37(8): p. 907–915.

83. Langmead B and Salzberg SL, Fast gapped-read alignment with Bowtie 2. Nat Methods, 2012. 9(4): p. 357–9. [PubMed: 22388286]

84. Love MI, Huber W, and Anders S, Moderated estimation of fold change and dispersion for RNA-seq data with DESeq2. Genome Biology, 2014. 15(12): p. 550. [PubMed: 25516281]

85. Gu Z, et al. , circlize implements and enhances circular visualization in R. Bioinformatics, 2014. 30(19): p. 2811–2812. [PubMed: 24930139]

86. Wu T, et al. , clusterProfiler 4.0: A universal enrichment tool for interpreting omics data. The Innovation, 2021. 2(3): p. 100141. [PubMed: 34557778]

Highlights

- Microglial Gi-Dreadd activation reduces acute KA-induced seizures.
- Gi-Dreadd activation increased microglia-neuronal interactions following seizures.
- Prolonged Gi-Dreadd activation arrests microglia in a homeostatic state.
- Chronic microglial Gi-Dreadd activation has detrimental seizure outcomes.

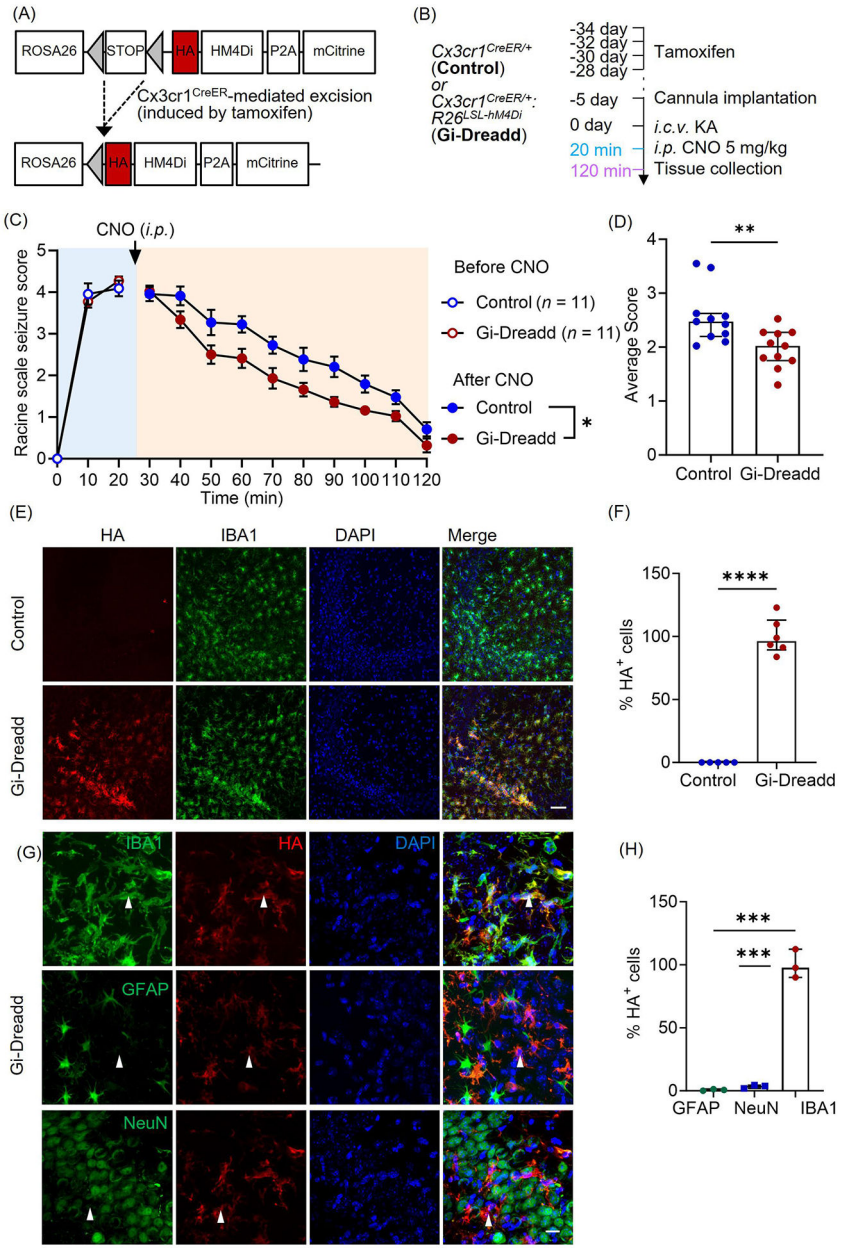

Figure 1: Chemogenetic modulation of microglia reduces seizure severity in the ICV-KA model of epilepsy.

(A) Generation of Cx3cr1$^{creER/WT}$: R26$^{LSL\text{-}hM4Di/WT}$ transgenic mice. (B) Experimental timeline for i.c.v. KA and CNO (i.p.) injection. (C) Seizure profile for mice that obtained a score of 3 and above in the first 20 min after KA administration. Results indicate that Gi-Dreadd activation by CNO reduced the severity of seizures (n =11/group). Analyzed by two-way ANOVA, mixed-effects model. Data represented as mean ± S.E.M. (D) Gi-Dreadd significantly reduced average seizure score. Analyzed by Mann-Whitney U test. (E) Representative images of IBA1 (green), DAPI (blue), and HA immunostaining (red) in the CA3 region of the hippocampus of Cx3cr1$^{creER/WT}$: R26$^{LSL\text{-}hM4Di/WT}$ mice (Gi-Dreadd) after tamoxifen. Scale bar, 50 μm. (F) HA expression co-localized with IBA1^{+} cells in

Gi-Dreadd mice, but not in Cx3cr1$^{creER/WT}$ (control). (G) Representative images of HA tag (red) colocalization with IBA1, NeuN, or GFAP (green) in the hippocampus of Gi-Dreadd mice. Scale bar, 15 μm. (H) Summarized results show HA was only co-localized with IBA1 positive cells. Analyzed by parametric t-test. Data represented as median with interquartile range, *p < 0.05, ** p < 0.01, *** p < 0.001.

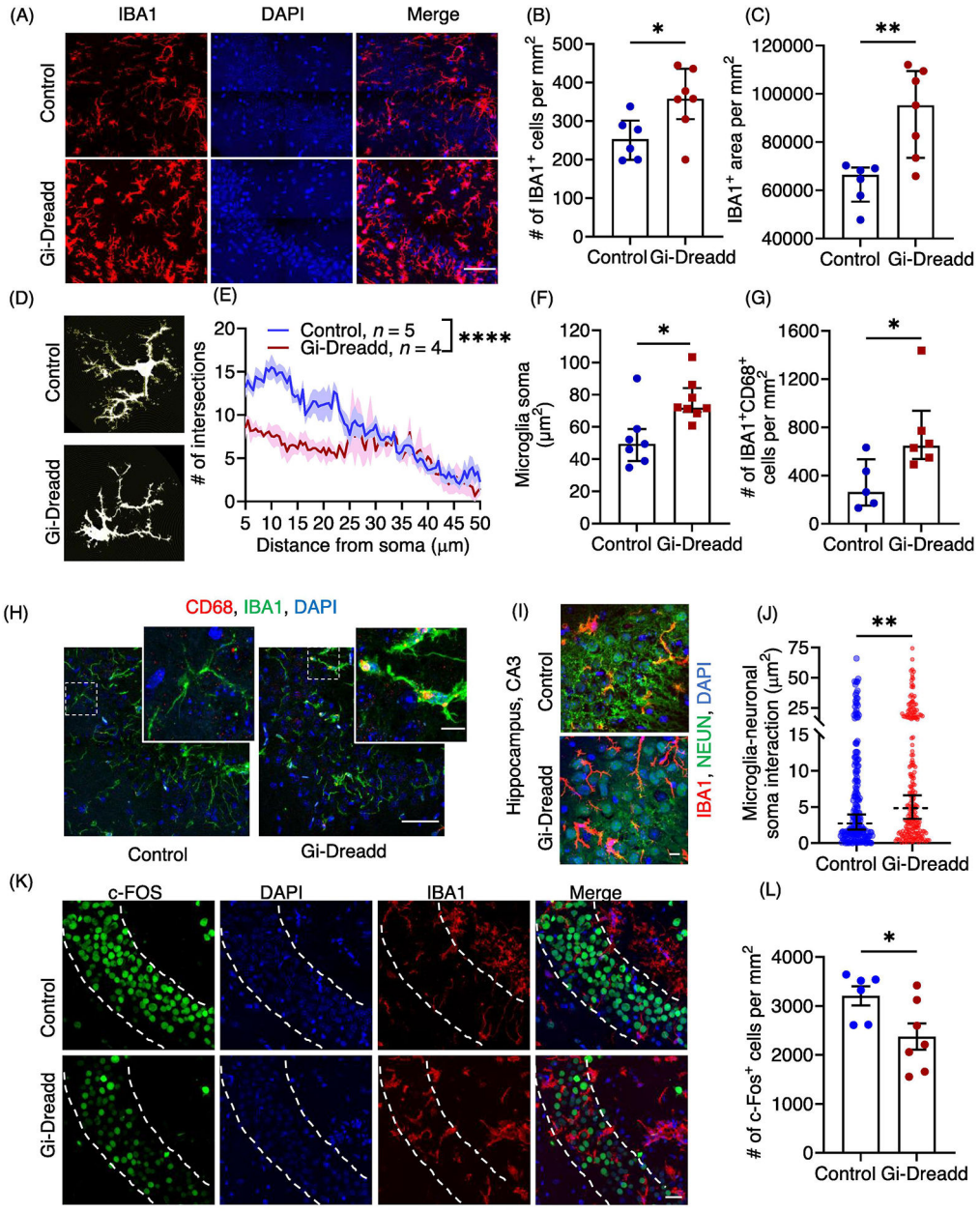

Figure 2: Acute activation of microglial Gi-Dreadd by CNO reduced neuronal hyperactivity following status epilepticus.

(A) Representative immunostaining images of IBA1 (red) and DAPI (blue) in CA3 region of hippocampus of Gi-Dreadd and control mice 2 h after KA administration. Scale bar, 50 μm. IBA1 positive cells (B) and IBA1 immunoreactive area (C) were increased in Gi-Dreadd when compared to control. (D) Representative images depicting morphological alterations in microglia. (E) Process complexity as determined by Sholl analysis. Analyzed by two-way ANOVA, mixed-effects model. (F) Gi-Dreadd activation increased microglial soma size. Analyzed by parametric t-test. (G) Gi-Dreadd activation increased number of $IBA1^{+}CD68^{+}$ cells with respect to controls. (H) Representative images of IBA1 (green), DAPI (blue), and CD68 (red) co-labelling in CA3 region of hippocampus, scale bar, 50 μm. Magnified

inset images showing co-localized CD68 expression with IBA1 (yellow), scale bar, 10 μm. (I) Representative images of microglia-neuronal soma interactions, scale bar, 10 μm. (J) Gi-Dreadd activation increased microglia interaction ($IBA1^+$ area) with Neuronal soma (each dot represents individual $NeuN^+$ ROI) when compared with controls following acute seizures. Analyzed using parametric t-test. (K) Representative images of c-FOS (green), IBA1 (red), and DAPI (blue), scale bar, 30 μm. (L) Gi-Dreadd activation reduced $c\text{-}FOS^+$ cell number following acute seizures when compared to control. Cell counts in both groups were compared using the Mann-Whitney U test (B, C, G &L). Data represented as median with interquartile range, *$p < 0.05$, ** $p < 0.01$, *** $p < 0.001$, **** $p < 0.0001$.

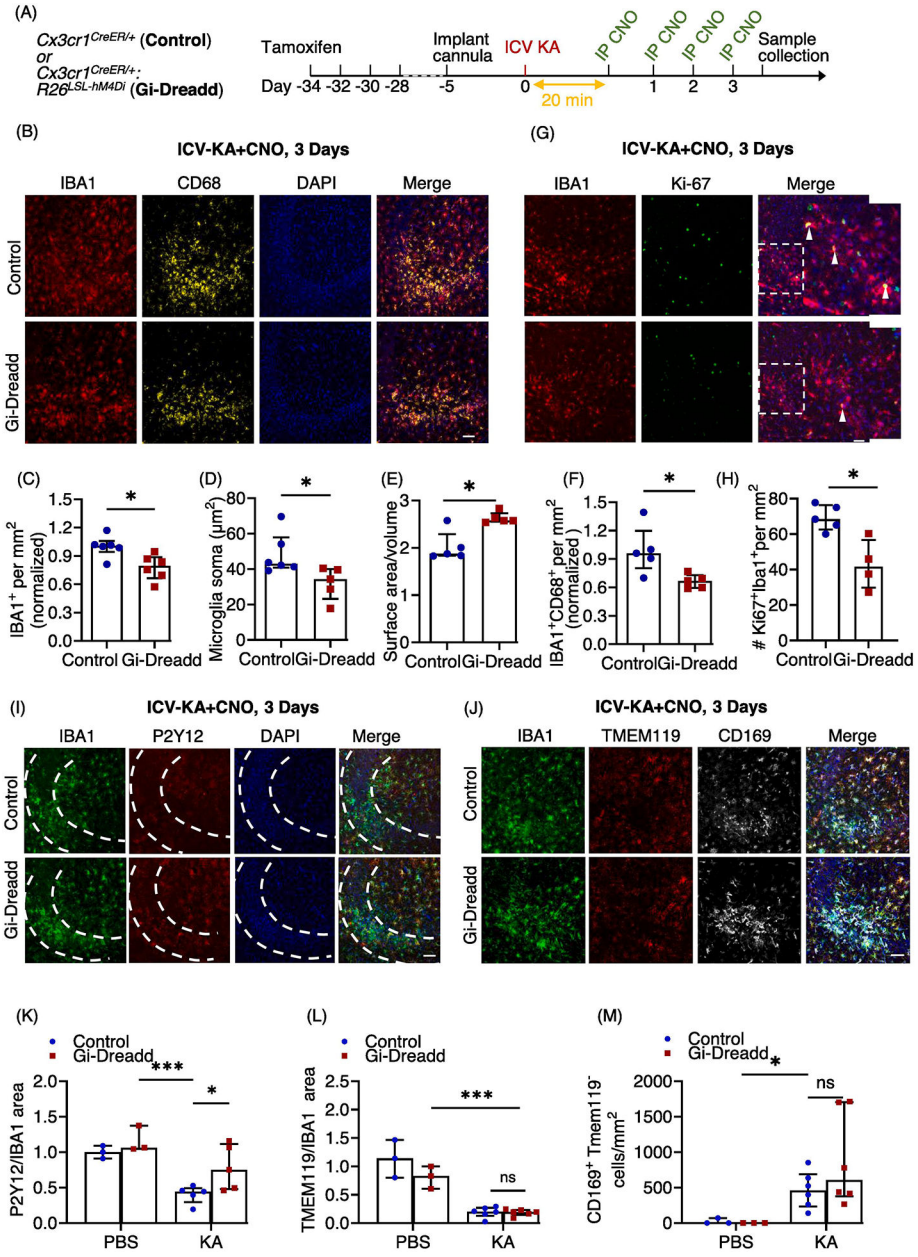

Figure 3: Prolonged activation of Gi-signaling by repeated CNO injections, arrests Gi-Dreadd expressing microglia in homeostatic-like state 3 days after i.c.v. KA induced SE.

(A) Experimental timeline. (B) Representative images of IBA1 (red), CD68 (yellow) and DAPI (blue) in the hippocampal CA3 region of Gi-Dreadd and Control mice. Scale bar, 50 μm. Prolonged activation of Gi-Dreadd signaling (C) decreased the number of $IBA1^+$ cells and (D) reduced microglial soma size when compared to controls. (E) Prolonged Gi-Dreadd activation increased morphological complexity of microglia. (F) Prolonged Gi-Dreadd activation reduced CD68 expression. (G) Representative images of IBA1 (red), Ki-67 (green) and DAPI (blue). Scale bar, 50 μm. (H) Prolonged Gi-Dreadd activation reduced the number of $Ki\text{-}67^+IBA1^+$ cells when compared to controls. (I) Representative images of IBA1 (green), P2Y12 (red) and DAPI (blue), scale bar, 50 μm. (J) Representative

images showing infiltrating monocytes in the CA3 region of hippocampus as determined by CD169 (grey), TMEM119 (red), IBA1 (green) and DAPI (blue) staining, scale bar, 50 μm. Cells which express CD169 but lack TMEM119 expression were considered as infiltrating macrophages. (K) Prolonged Gi-Dreadd activation increased the ratio of P2Y12 area per IBA1 area when compared to control. (L) No difference in the ratio of Tmem119 area per IBA1 area between groups. (M) No difference in the number of $CD169^{+}TMEM119^{-}$ cells between groups. All groups were compared using the Mann-Whitney U test. Data represented as median with interquartile range, *$p < 0.05$, ** $p < 0.01$, *** $p < 0.001$.

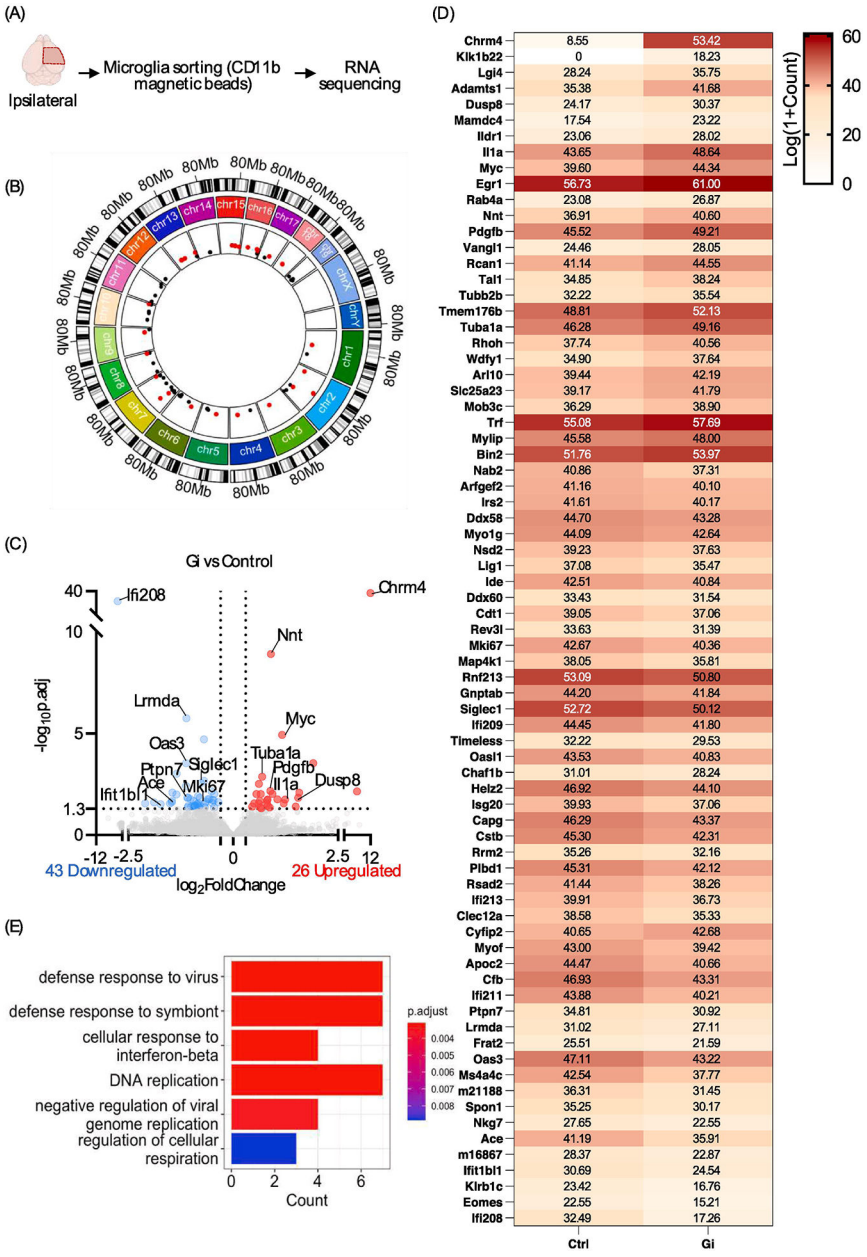

Figure 4: Transcriptomic alterations in microglia upon prolonged Gi-signaling activation following status epilepticus.

(A) Overview of RNAseq experiment design. (B) Visualization of differentially expressed gene (DEG) chromosomal locations. Upregulated DEGs are labeled pink and downregulated DEG are labeled black. (C) Volcano plot of DEGs. Threshold: *p.adj <0.05*, *|log2 fold-change| > 0.5*. (D) Heatmap of each DEG. Relative expression: *Log(1+Count)*. (E) Boxplot of significant GO pathways.

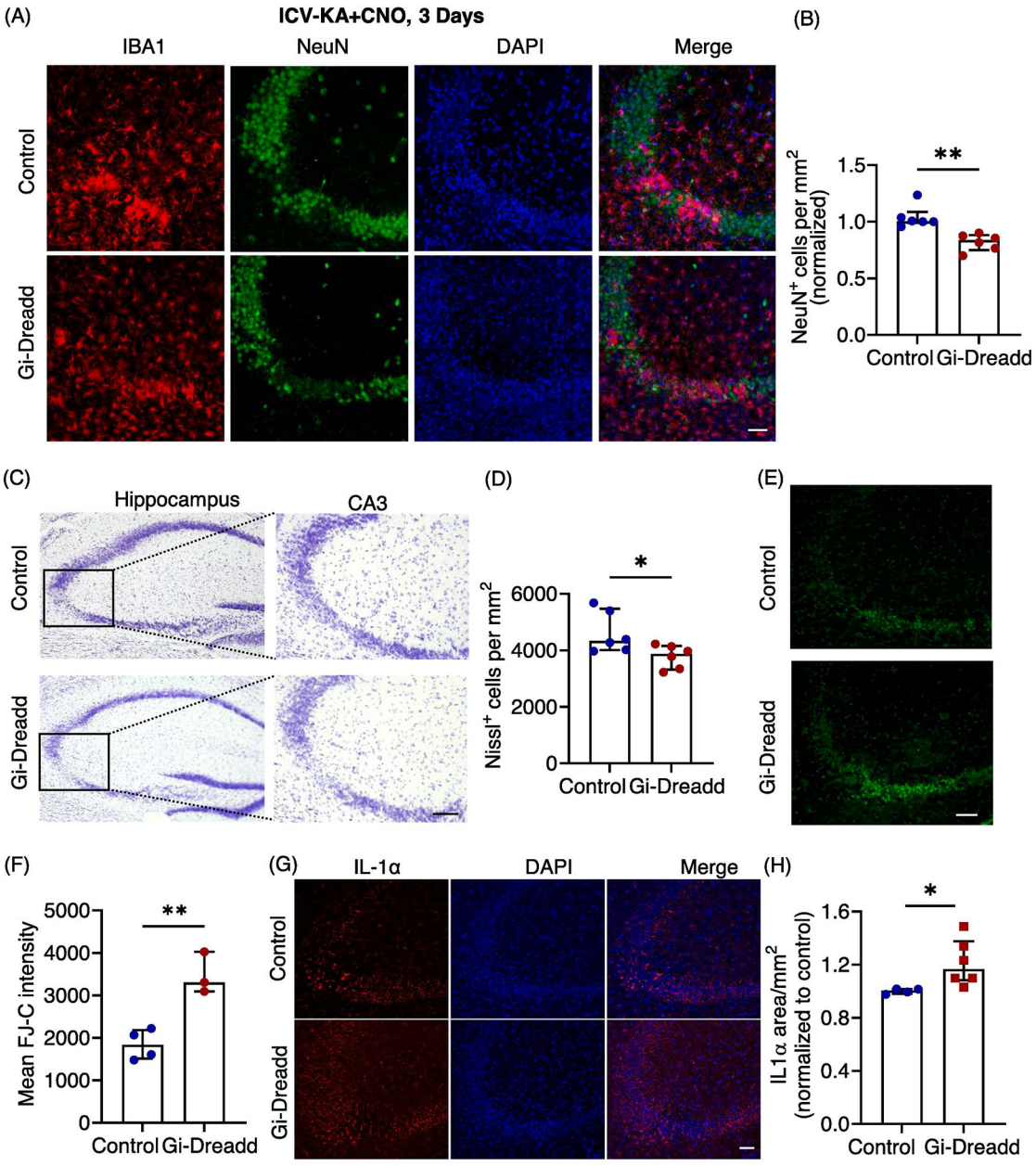

Figure 5: Prolonged microglial Gi-Dreadd activation increases neuronal death.

(A) Representative images of IBA1 (red), NeuN (green) and DAPI (blue) in the hippocampal CA3 region of Gi-Dreadd and Control mice 3 days after KA administration, scale bar, 50 μm. (B) Prolonged Gi-Dreadd activation reduced $NeuN^+$ cells density when compared to controls. (C) Representative Nissl staining images, scale bar, 50 μm. (D) Prolonged Gi-Dreadd reduced the number of Nissl positive cells. (E) Representative images of Fluoro Jade-C (FJ-C) staining, scale bar, 50 μm. (F) Prolonged Gi-Dreadd activation increased the number of FJ-C positive cells relative to controls. Analyzed by parametric t-test. (G) Representative images of IL-1α (red) and DAPI (blue), scale bar, 50 μm. (H) Gi-Dreadd increased IL-1α immunoreactivity when compared with controls. Cell counts in both

groups were compared using the Mann-Whitney U test. Data represented as median with interquartile range, *p < 0.05, ** p < 0.01, *** p < 0.001.

Table 1:

Top GO terms identified by GSEA.

GO term ID	Description	$P_{adj.}$
GO:0035456	response to interferon-beta	0.000499
GO:0009615	response to virus	0.000809
GO:0051607	defense response to virus	0.000809
GO:0140546	defense response to symbiont	0.000809
GO:0002253	activation of immune response	0.002313
GO:0035458	cellular response to interferon-beta	0.002914
GO:0045089	positive regulation of innate immune response	0.008068
GO:0002833	positive regulation of response to biotic stimulus	0.008068
GO:0050778	positive regulation of immune response	0.009191
GO:0002831	regulation of response to biotic stimulus	0.011588
GO:0002218	activation of innate immune response	0.015124
G0:0045088	regulation of innate immune response	0.015124
GO:0060700	regulation of ribonuclease activity	0.019769
G0:0072111	cell proliferation involved in kidney development	0.019769
G0:0000819	sister chromatid segregation	0.024317
G0:0009111	vitamin catabolic process	0.024678
G0:0032069	regulation of nuclease activity	0.030627
G0:0007059	chromosome segregation	0.035118
G0:0006281	DNA repair	0.041036
GO:0030550	acetylcholine receptor inhibitor activity	0.044216
G0:1901722	regulation of cell proliferation involved in kidney development	0.048093

Table 2:

List of Antibodies

Name	Company	Cat#	Species	Dilution
Iba-1	Abcam	Ab104225	Rabbit	1:500
Iba-1	Wako	011–27991	Goat	1:300
CD68	Abcam	Ab125212	Rabbit	1:500
TMEM119	Abcam	209064	Rabbit	1:300
c-fos	CST	2250S	Rabbit	1:500
NeuN	Abcam	Ab104225	Rabbit	1:500
NeuN	Abcam	Ab104224	Mouse	1:500
GFAP	CST	3670s	Mouse	1:500
P2Y12	Anaspec	As55043A	Rabbit	1:400
CD169	BIO-RAD	MCA884	Rat	1:400
Ki67	Santa Cruz	Sc23900	Mouse	1:300
Anti-HA-Peroxidase	Roche (Sigma-Aldrich)	23551600 (Clone 3F10)	Rat	1:200
GFP	Aves Labs	GFP-1010	Chicken	1:1000
IL-1 beta	Cell signaling	12242S	Mouse	1:400
IL-1 alpha	Abcam	Ab7632	Rabbit	1:200